Leakage Error Analysis in Isolated Superconductor Multi-State Qubit Transmon

Krajnç Lõvren [1], Ahmad M. Abdullah [1,2*], Şkalar Radiç [1]

[1] Department of Applied Materials Science, Faculty of Applied Sciences, University of Ljubljana, Ljubljana, SLOVENIA
[2] Department of Physics, College of Education, Thi Qar University, Nasiriyah, IRAQ
[*] Corresponding author email: abdullah2311975@yahoo.com

Abstract
In this letter, experimental results of an isolated superconductor qubit transmon are presented. The carrier frequency is scanned within a wide bandwidth covering resonances with higher states and then the leakage probabilities are measure by sensitive measuring protocols. The experimental data were compared to typical predictions to determine the active leakage rates and dangerous resonance bandwidth. This work may provide a quantum understanding and base for one of the important error sources in the digital quantum computing to achieve much more reliable systems.

Keywords: Quantum dots; Photoluminescence; Resonance modes; Multimode cavities
Received: December 2025; **Revised:** January 2026; **Accepted:** February 2026; **Published:** April 2026

1. Introduction

The transmon qubit represents the cornerstone in many modern quantum computing platforms, especially those are based on superconductor circuits due to their relatively long coherence times and reproducibility [1]. Fundamentally, this qubit operates as an active system of two levels in the multi-dimension Hilbert space where the standard states (⟨0| and ⟨1|) are defined as the basic and excited states of the fundamental oscillation in the transmon phase [2]. However, transmon is a multi-level nonlinear system in which, the higher states, such as ⟨2|, ⟨3| or higher, are included in its spectrum. The ability to perform reliable control processes on ⟨0| and ⟨1| states without leakage to the higher states is called the inclusion [3]. Such leakage is a source for an error exceeding the qubit errors occurring inside the subspaces of the two states [4]. It can severely degrade the performance of the quantum algorithms, especially the long ones or those depend on the quantum correction of errors where error rates are required to be lower than specific thresholds [5]. This study aims to accurately characterize the leakage losses in a transmon qubit when digital control pulses are applied with their carrier frequencies in resonance with specific energy gaps between the higher quantum states [6]. This would convert the common unintended mode of leakage resulted from wide frequency bandwidth into a most dangerous state of intended and modified leakage throughout resonance [7].

In order to understand the mechanisms of this resonance leakage, it is important to explore a comprehensive Hamiltonian model of controlled transmon. The unperturbed transmon is described as a series of inharmonic energy states with contradicted energy gaps, i.e., $E_{01}>E_{12}>E_{23}$ [8]. Usually, this can be controlled by a microwave signal applied to the entrance of the transmission line or to the transformation gate, which leads to a potential-like interaction. After performing a rotating wave approximation on the pulse carrier frequency, the perturbation resulted from this pulse is usually described by some conditions leading to transitions among the states [9]. The common simplification is the assumption that the pulse amplitude is weak and its frequency is close to the frequency of the fundamental transition (ω_{01}), which leads to an active Hamiltonian between the states. In such model, the transitions to higher states (e.g., $\langle 0| \rightarrow \langle 2|$) are approximately forbidden because it requires the generation of photons with frequency of $\omega_{02}=2\omega_{01}-\eta$, where η is the anharmonicity parameter, which is not exist in the spectrum of the single frequency pulse. Here, this leakage is considered as a secondary result of a side frequency content or pulse deformation [10].

The practical consequences of such type of leakage errors are severe. First, they impose uncorrected errors in the calculations as the leakage to ⟨2| state cannot be corrected by the quantum correction symbols designed for qubit errors [11,12]. Second, even the qubit returns later to the computing space, it may return with a random-phase state, and then transform the leakage error to a much complex logic error. Third, the dynamics at the higher states (such as $\langle 2| \rightarrow \langle 1|$ transition) via spontaneous emission lead to wrong intervals and then increase the data recovery time [13]. In multi-qubit systems, the

leakage may propagate throughout couplings that deform the adjacent qubits. Therefore, the understanding of resonance leakage maps is not a theoretical practice but a frequency-aware compilation in the quantum translators, to enhance frequencies in multi-qubit treatments, and finally to design much more powerful control protocols [14].

In this letter, experimental results of an isolated superconductor qubit transmon are presented. The carrier frequency is scanned within a wide bandwidth covering resonances with higher states and then the leakage probabilities are measure by sensitive measuring protocols. The experimental data were compared to typical predictions to determine the active leakage rates and dangerous resonance bandwidth. This work may provide a quantum understanding and base for one of the important error sources in the digital quantum computing to achieve much more reliable systems.

2. Experimental Part

Based on the practical scheme shown in Fig. (1), which is proposed to study the leakage errors in transmon qubit systems those are resulted from the resonant digital control, such system is described by three main parts: physical, technical, and analytical.

This system is based on the transmon slide placed in dilution refrigerator at low temperatures (down to 4 mK) to ensure the stability of the quantum state and reduce thermal noise. This system shows a precise interaction between transmon energy states concentrated on the undesired transition from computing states, such as ⟨g| and ⟨e|), to higher states, such as ⟨f|. this system is controlled via multiple paths including magnetic flux control lines to adjust the qubit frequency using SQUID technique, as well as XY control responsible to rotating quantum states. The goal of this environment is to isolate the qubit completely with accurate digital signals allowed to reach the nano-conductors in order to study the effect of resonance digital pulses, which may cause energy leakage to states outside the dual domain of the computing. This is the largest challenge in the stability of the superconductor quantum processors.

The system contains a modern digital control unit (FPGA/DAC) to generate control pulses at an extremely high temporal accuracy. The main feature is the use of resonance digital control as the frequency (ω_d) is adjusted to be close the transition frequency between the "e" and "f" states (ω_{ef}), which is called the resonant impulsion. These signals pass through a series of pulse modulators and amplifiers before entering the cooled medium via low-pass filters to ensure the signal purity. These digital pulses are designed to represent logic gates but due to the weak inharmonic nature of transmon, the pulses of wide bandwidth or interfered frequencies may stimulate the transitions to the "f" state. The system is designed to measure the efficiency of the digital gates to reduce the leakage when compared to the conventional control as the gate time (τ_{gate}) as a crucial parameter in balancing errors.

The system is completed by a readout system depending on resonator/cavity transmission related to the qubit as the qubit state affects the cavity resonance frequency. The readout pulse is transmitted through the qubit and pick the data. This weak signal is then reasonably amplified using low-noise amplifiers (such HEMT) and band-pass filters before reaching the digitizer at the data analysis unit. The analytical power of this system can be seen in its ability to distinguish between the three states (g, e, and f) throughout digital signal processing to allow the researchers to characterize the leakage rate with high statistical accuracy. Finally, these data are linked to analysis and data acquisition to compare the practical performance to the theoretical models [15,16]. This would allow understanding how the shape and frequency of digital pulse affect the quantum information integrity and prevent their loss in the undesired higher energy states.

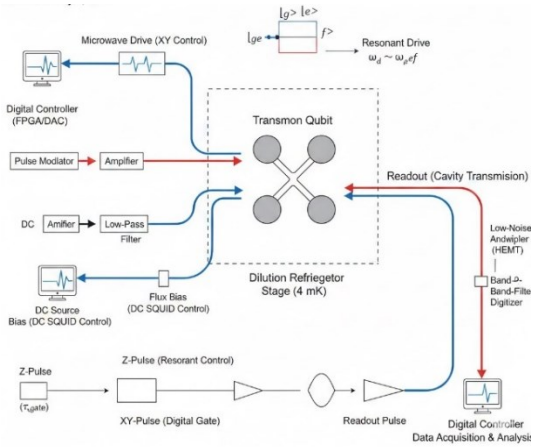

Fig. (1) The proposed experimental scheme: characterization of leakage errors in a transmon qubit due to resonant digital control

3. Results and Discussion

Figure (2) shows the dynamics of the second excited state ⟨2| represented by P_2 as a function of delay time after setting the qubit in ⟨1| state at zero time. The data show apparent non-periodic behavior as a fast initial increase in P_2 followed by an exponential decrease to a low equilibrium value. This behavior indicates two contradicting mechanisms affecting the population in a multi-level qubit. Within the first stage, with an initial increase, the system is excited from ⟨1| state to ⟨2| state. During delay time of 0-30 μs, the value of P_2 increased from 0.3% to its peak value of 1.7%. This clearly refers to the existence of an active pumping channel transforming the qubit state from ⟨1| to ⟨2|. The possible mechanisms are the reverse relaxation, relaxation via

an intermediate, or transmon-mediated relaxation. The reverse relaxation is possible under thermal unbalance conditions or due to non-mutual coupling with the surrounding, such as photonic noise of suitable frequency to transfer from ⟨1| to ⟨2|, i.e., ω_{12}. The relaxation via an intermediate is indirect transition from ⟨1| to ⟨2| throughout coupling with surrounding at other degrees of freedom, such as dual-state defects. By the transmon-mediated relaxation in the multi-level qubits, relaxation may transfer to an adjacent qubit. The peak at about 30 μs indicates that the pumping rate to the ⟨2| state is initially higher than relaxation rate from this state to a lower state.

In the second stage of exponential decrease (30-100 μs, the system returned to thermal equilibrium state. Beyond the peak, P_2 began to decrease exponentially to a low steady value (~0.15%) at 100 μs. This reveals that the relaxation rate from ⟨2| to ⟨1| dominates after saturation. The relaxation from ⟨2| occurs throughout two routes. The first is ⟨2|→⟨1| at a rate of Γ_{21} with emitted photon of ω_{12} frequency. The second is ⟨2|→⟨0| at a rate of Γ_{20} (directly via a dual-photon transition or via ⟨1| as an intermediate state). The low steady value (0.15%) coincides the population of ⟨2| state at thermal equilibrium, which can be estimated by Boltzmann distribution [17]:

$$P_2^{th} \approx e^{-\hbar\omega_{02}/k_B T} \quad (1)$$

where ω_{02} is the transition frequency between ⟨0| and ⟨2| states, the very low value refers to a very low temperature of the surrounding environment ($T \ll \hbar\omega_{02}/k_B$)

The dynamics between ⟨0| and ⟨1| states can be indirectly concluded from the conservation probability:

$$P_0 + P_1 + P_2 = 1 \quad (2)$$

At time = 0, $P_0 \approx 0$, $P_2 \approx 0.003$, $P_1 \approx 1$. At the peak (30 μs), P_1 started to decrease due to relaxation to ⟨0| as well as pumping to ⟨2|. At longer times, the system reached steady state throughout thermal equilibrium, where $P_0 \approx$ 0.98-0.99 (ground state), $P_1 \approx$ 0.01-0.02 (first excited state), and $P_2 \approx$ 0.0015 (second excited state).

Results showed that idling durations can cause reasonable leakage to the ⟨2| state, not throughout direct control, but throughout pumping-relaxation mechanisms. This affects the quality of the consecutive gates and increases the error rate. This problem can be solved by determining the source of noise causing the transfer from ⟨1| to ⟨2|, such as charge noise and parasitic photons. It can be also be solved by modifying idling time. In quantum algorithms, the short idling time should be avoided around the peak time (30 μs) as much as possible. The active cooling protocols can be used to solve the problem. Active cleanup and reset pulses can be used to restore the population of the ⟨0| state after long idling times [18].

Comparing to the theoretical models, the obtained results provide an accurate calibration curve for the transition rates as follows. The pumping rate ⟨1|→⟨2| is determined from the scope of the initial increase. The relaxation rate ⟨2|→⟨1|/⟨0| is determined from the time constant of the exponential decrease (relaxation time T_1 of the active state ⟨2|).

The results show clearly a dynamic competition between pumping mechanism (filling ⟨2|) and relaxation mechanism (depopulating ⟨2|). Understanding this behavior is crucial to enhance the qubit stability, reduce the spontaneous leakage errors, and increase the accuracy of quantum processes in transmon systems. The problem of leakage to higher states is not only related to the pulse control, but to the idling and thermodynamic states of the system. Consequently, this requires comprehensive multi-state control strategies.

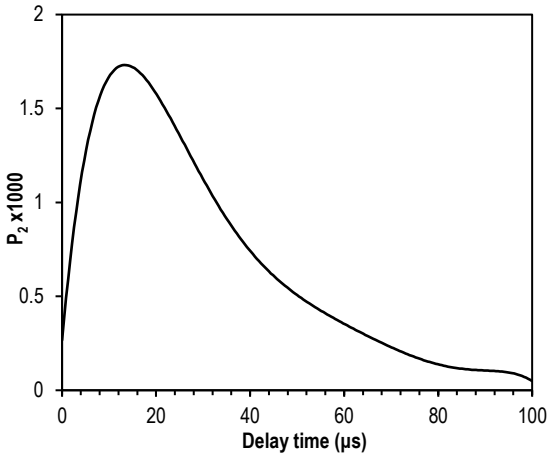

Fig. (2) The dynamics of the second excited state ⟨2| represented by P_2 as a function of delay time after setting the qubit in ⟨1| state at zero time

Figure (3) shows the behavior of spontaneous relaxation of qubit from the excited state ⟨1| (black line) to the ground state ⟨0| (red line) as a function of delay time. An apparent exponential decrease in the existence probability of qubit at ⟨1| state in synchronization with increase in the probability of ⟨0| state. This behavior represents the critical physical parameter (T_1), which is the time taken by the qubit to lose its energy and return to the steady state due to the interaction with the surrounding environment or thermal noise. The intersection point between the two curves at about 15 μs refers to the moment at which the system can equally exist at both states. This is a direct indication of decoherency in such experimental quantum system.

These curves are not merely raw data, but a result of fitting using the rate equations mentioned before. These curve reveal the capability of the theoretical model to simulate the experimental behavior at high accuracy over time range of 0-100 μs. Fitting allows the extraction of accurate values for the transition

constants. It is assumed that the variation rates of populations in P_0 and P_1 follow a first-order differential equation. At long times (~100 μs), the probability of ⟨0| state is close to unity whereas the probability of ⟨1| state completely vanishes. This confirms that the system reaches the thermal-equilibrium ground state, which is the expected result of relaxation processes in superconducting qubit systems.

With searching for leakage errors, this chart can be considered the base to evaluate the digital control efficiency. If there is large leakage to the higher states (⟨2| or ⟨f|), the summation of probabilities P_0+P_1 will not perfectly equal to 1 over time, otherwise, deviations will appear in the exponential behavior. The precise fitting of rate equation explains that the system still reasonably confined inside the dual-state space (⟨0| and ⟨1|) during free relaxation process. Therefore, the challenge is how the resonant digital control of leakage is activated while the logic gates are applied [19]. So, this chart represents the baseline through which the deviation of qubit from the ideal behavior is measured when subjected to intense resonant digital control pulses.

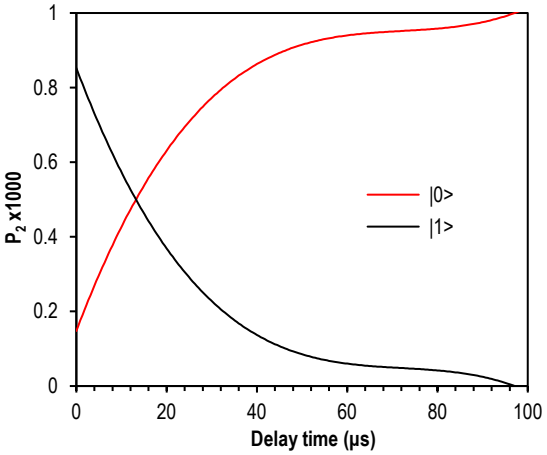

Fig. (3) The behavior of spontaneous relaxation of qubit from the excited state ⟨1| (black line) to the ground state ⟨0| (red line) as a function of delay time

4. Conclusion

In conclusion, experimental results of an isolated superconductor qubit transmon were compared to typical predictions to determine the active leakage rates and dangerous resonance bandwidth. This work may provide a quantum understanding and base for one of the important error sources in the digital quantum computing to achieve much more reliable systems.

References

[1] A. ur Rehman et al., "A comparative study of the photonic crystals-based cavities and usage in all-optical-amplification phenomenon", *Photon. Nanostruct. Fundam. Appl.*, 61 (2024) 101298.

[2] U. Zamir et al., "Intracavity laser absorption spectroscopy: Performance and advantages for energy science", *Appl. Energy Combus. Sci.*, 17 (2024).

[3] T. Jennewein et al., "QEYSSat 2.0—white paper on satellite-based quantum communication missions in Canada", *Canad. J. Phys.*, 103(4) (2024) 328-376.

[4] D.-R. Li et al., "Single nanowire integrated microfiber devices", *Result Opt.*, 5 (2021) 100199.

[5] S. Weigl et al., "Photoacoustic detection of acetone in N_2 and synthetic air using a high power UV LED", *Sens. Actuat. B: Chem.*, 316 (2020) 128109.

[6] E. Desurvire et al., "Science and technology challenges in XXIst century optical communications", *Comptes Rendus Physique*, 12(4) (2011) 387-416.

[7] S. Shahid, S.-E. Zumrat and M.A. Talukder, "A merged lattice metal nanohole array based dual-mode plasmonic laser with an ultra-low threshold", *Nanoscale Adv.*, 4(3) (2022) 801-813.

[8] F. Pilat et al., "Hot-cavity linewidth enhancement factor of a quantum cascade laser", *Opt. Laser Technol.*, 182(B) (2025) 112112.

[9] S. Mikki, "Theory and computation of Markovian quantum antenna systems", *Result Phys.*, 49 (2023) 106453.

[10] F.D. Santillan and A. Hanke, "Rabi oscillations and entanglement between two atoms interacting by the Rydberg blockade studied by the Jaynes–Cummings Model", *Phys. Open*, 24 (2025) 100292.

[11] S. Castelletto et al., "Deterministic placement of ultra-bright near-infrared color centers in arrays of silicon carbide micropillars", *Beilstein J. Nanotech.*, 10 (2019) 2383-2395.

[12] G. Heinrich et al., "Dynamics of coupled multimode and hybrid optomechanical systems", *Comptes Rendus Physique*, 12(9-10) (2011) 837-847.

[13] S. Berneschi et al., "From laboratory to prototype: the last-mile issue in whispering gallery mode resonator-based devices", *Opt. Mater.*, 167 (2025) 117248.

[14] G.H.M. van Tartwijk and G.P. Agrawal, "Laser instabilities: a modern perspective", *Prog. Quantum Electron.*, 22(2) (1998) 43-122.

[15] R.-R. Meng et al., "Solid-state quantum nodes based on color centers and rare-earth ions coupled with fiber Fabry–Pérot microcavities", *Chip*, 3(1) (2024) 100081.

[16] J. Wekalao et al., "Machine learning-driven terahertz graphene-MXene-gold metasurface biosensor for dual COVID-19 and cervical cancer biomarker detection", *Sens. Bio-Sens. Res.*, 50 (2025) 100920.

[17] P. Hautle and W.Th. Wenckebach, "Creating high, portable proton polarization with photo-excited triplet DNP", *J. Mag. Resonance Open*, 20 (2024) 100159.

[18] J. Zhu and J. Lou, "High-sensitivity Fano resonance temperature sensor in MIM waveguides coupled with a polydimethylsiloxane-sealed semi-square ring resonator", *Result Phys.*, 18 (2020) 103183.

[19] O. Melchert et al., "Two-color soliton meta-atoms and molecules", *Optik*, 280 (2023) 170772.

